6A.1 LARGE-SCALE INFLUENCES ON THE GENESIS OF HURRICANE KARL (2010)

Kyle S. Griffin and Lance F. Bosart
Department of Atmospheric and Environmental Sciences, University at Albany/SUNY, Albany, NY

1. INTRODUCTION

The events leading up to the genesis of Hurricane Karl (2010) pose a unique opportunity to examine the continuing problem of understanding tropical cyclogenesis. A precursor disturbance to the genesis of Karl was well sampled by the PRE-Depression Investigation of Cloud-systems in the Tropics (PREDICT). Dropsonde observations obtained in PREDICT provide a means to examine the pre-genesis environment of Karl in great detail, specifically via improved gridded analyses. The disturbance that became Karl (hereafter, pre-Karl) formed east of the Leeward Islands early on 9 September and moved slowly westward through late 10 September, when it began organizing. At this point, pre-Karl moved west-northwest until becoming a tropical cyclone at 1200 UTC 14 September. This presentation examines the genesis of the precursor disturbance from both a synoptic and equatorial wave perspective and suggests that the two perspectives are inherently linked.

The term ‘synoptic’ perspective refers to the focus on synoptic-scale features and flow patterns with a frequency of a few days that have been examined by both operational forecasters and researchers in the tropics for decades. The term ‘equatorial wave’ perspective focuses on convectively coupled equatorial waves (CCEWs), first described by Matsuno (1966), that occur on intraseasonal time scales. CCEWs modulate tropical convection on lower temporal frequencies than are observed with synoptic-scale features. With these definitions in mind, the genesis of the pre-Karl disturbance is examined from both perspectives in an effort to demonstrate that some observable synoptic-scale features are likely associated with CCEW activity.

2. DATA AND METHODS

The 0.5 degree Climate Forecast System Reanalysis (CFSR; Saha et al 2010) gridded dataset was employed for the synoptic perspective because PREDICT dropsondes were incorporated into the data assimilation process. CFSR data are used in conjunction with filtered outgoing longwave radiation (OLR) and Tropical Rainfall Measuring Mission (TRMM) rain rate measurements to track CCEW features for the equatorial wave perspective. These satellite-derived measurements are further processed by applying the CCEW filtering techniques of Wheeler and Kiladis (1999) and Kiladis et al (2006). Lastly, ERA-Interim data are used for compositing purposes.

3. SYNOPTIC PERSPECTIVE

One of the major players in the initial spin-up of the pre-Karl disturbance is a surge of southerly winds from northern South America on 8-9 September. Low-level vorticity increases on the western cyclonic shear side of this wind surge. This low-level vorticity results in the generation of a briefly closed earth-relative circulation near the southern Leeward Islands and serves to substantially increase local convective activity into 10 September. However, this circulation weakens late on 10 September and remains weak until late on 12 September, during which time the disturbance lacks vertical organization and only sporadically produces convective bursts. During 13-14 September, more persistent convection develops as the disturbance

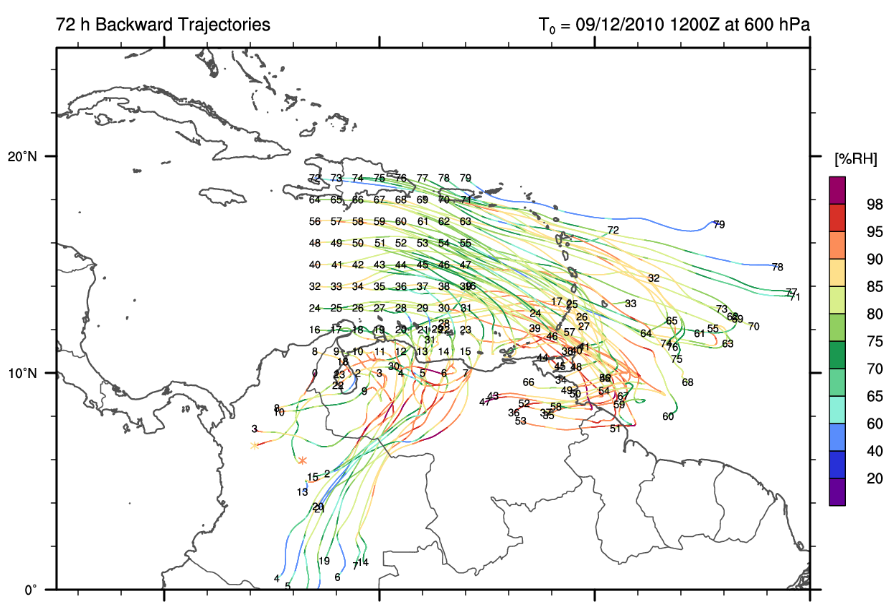

FIG 1. 72 hour backward trajectories computed from 1200 UTC 12 September 2010 and an initial level of 600 hPa on a 1˚ grid centered on the location of the pre-Karl disturbance. Colors along the track indicate the relative humidity of the parcel.

becomes vertically stacked and pre-Karl was classified as a tropical storm at 1200 UTC 14 Sept.

3.1 *Trajectory Analysis*

During the initial spin-up of the pre-Karl disturbance, two distinct air masses dominated the surrounding environment. To the north and east, a dry air outbreak dominates the mid-levels (700-500 hPa), while the aforementioned southerly wind surge begins to influence the southern portions of the disturbance. Numerous trajectories were calculated to analyze the interaction between the pre-Karl disturbance and these air masses. Forward trajectories from the dry air mass shows many of the parcels slowly moistening as they reaches the northern fringes of the disturbance, suggesting the relatively dry air contributed to the intermittent nature of the convection throughout the pre-genesis life cycle of the disturbance.

Similarly, backward trajectories were calculated from a grid encompassing the pre-Karl disturbance at various points in its life cycle. These trajectories reaffirm the presence of dry air along the northern periphery of the system as well as highlight a well-focused stream of air from northern South America (a sample set of trajectories can be seen in Fig. 1). While present throughout the entirety of the low- and mid-levels (through 600 hPa), the southern trajectories appear to be funneled by the northern Andes and down the Orinoco River valley of Venezuela. As early as 10 September, this southern airstream appears to be transporting relatively dry air towards the developing tropical disturbance, further hindering the development of persistent convection.

By 12 September, trajectories from the southerly wind surge begin to indicate that moister air is being transported towards the disturbance (not shown). While it is difficult to make a conclusive argument from trajectory analyses alone, it is reasonable to assume that air parcels reaching the southern Caribbean from the south became increasingly moist between 10 and 12 September, helping to make the environment more favorable for persistent convective activity.

A more detailed look at the origin of the southerly wind surge shows that the surge originates as strong southeasterly flow over the subtropical Amazonian basin. However, no mid-latitude trough is immediately apparent as a precursor to this surge, despite previous literature suggesting a mid-latitude influence is common with CCKW events over South America (e.g. Liebmann et al 2009). This leads to a further investigation of the CCEW environment surrounding the genesis of the pre-Karl disturbance.

4. EQUATORIAL WAVE PERSPECTIVE

CCEWs appear to play a significant role in the development of the pre-Karl disturbance. Specifically, the passage of a convectively coupled Kelvin wave (CCKW) propagating eastward over northern South

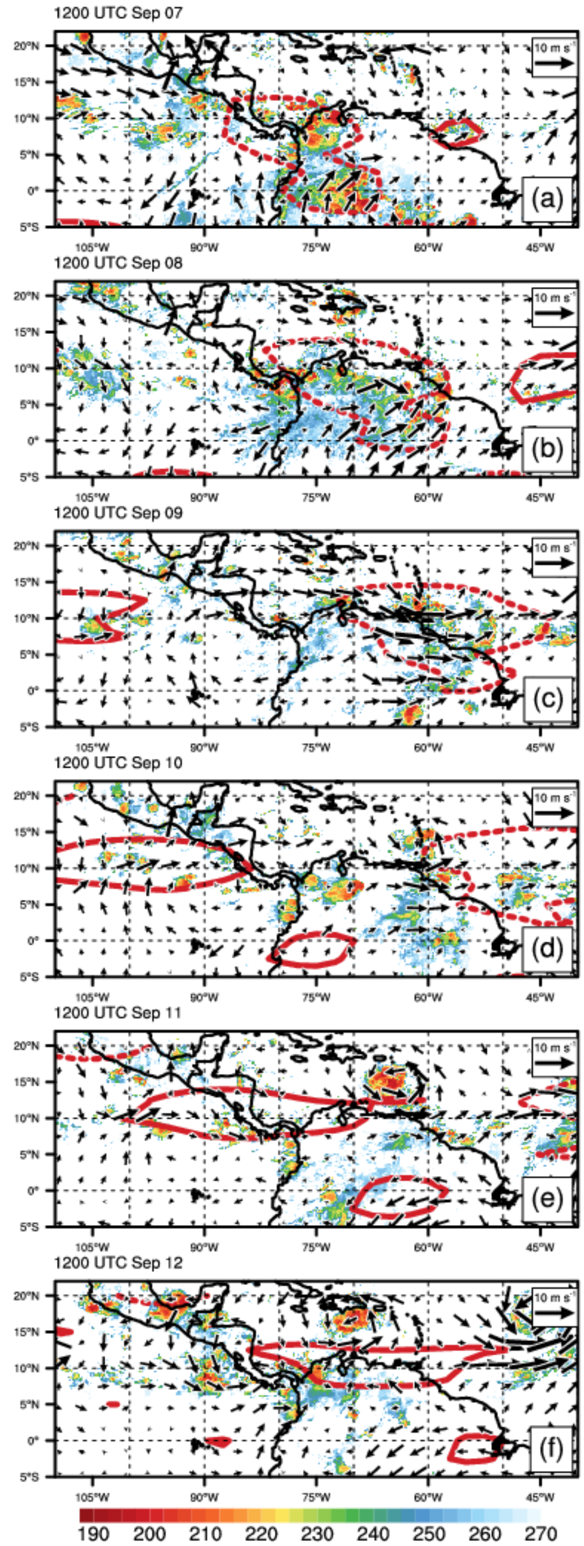

FIG. 2. Infrared imagery (shaded) overlayed with anomalous 850 hPa winds (vectors) and CCKW-filtered OLR anomalies (only the 12 W m^{-2} contour; red; negative anomalies [active phase] dashed) at 1200 UTC 7-12 September 2010.

America on 7-9 September (Fig. 2a-c) leads to an enhancement of convection across the region. Ahead of the CCKW, a small region of showers can be observed near 55˚W (Fig. 2a), the first sign of the pre-Karl disturbance. As the CCKW begins to interact with these showers, convective activity increases noticeably (Fig. 2b-c). This convection persists and remains well organized after the passage of the CCKW (Fig. 2d) before becoming increasingly intermittent through 11-12 September.

This relatively rapid organization of the pre-Karl disturbance during 9-11 September can be attributed, at least in part, to a number of environmental conditions associated with the environment after the passage of the convectively active phase of a CCKW. Ventrice et al (2012; in press) show that tropical cyclogenesis frequency increases 1-2 days after the passage of a CCKW. Ventrice et al state that the increase in tropical cyclogenesis frequency is related to an ~1.5 m s^{-1} decrease in the climatological westerly wind shear in the region. Further, Schreck and Molinari (2011) show that the convectively active phase of a CCKW also leaves behind a ribbon of enhanced low-level cyclonic vorticity, which can then be observed to break down into vortices and eventually form tropical cyclones.

While not the specific focus of this discussion, it should also be noted that the suppressed phase of the CCKW passed across the Caribbean and northern South America on 12-13 September (Fig. 2e-f). The timing of this passage is associated with an increase in the range of the diurnal convective activity of the pre-Karl disturbance (Montgomery et al. 2012), suggesting the convective struggles of the disturbance during these two days may have been associated with the unfavorable CCEW state.

4.1 *CCKW-based composites*

While both the synoptic and equatorial wave perspectives have been presented separately, there is no obvious reason why either of these perspectives should remain separate from the other. In an attempt to combine the two perspectives, a series of time-lagged composites were created to investigate any possible relationship between CCKW activity over northern South America and the observed meridional wind flow from over the Amazon. These composites are similar to those presented in Liebmann et al (2009). Composites were created to examine the association between CCKW activity and anomalous meridional winds over subtropical South America, the source of the aforementioned southerly wind surge. Since the relationship of interest involves cases that could potentially affect tropical cyclogenesis, composites were created based on the July-October 1998-2010 period using CCKW-filtered TRMM anomalies greater than one standard deviation above the mean. These data were calculated using an average over 5-10˚N at a base longitude of 70˚W in an attempt to capture the events of most significance to potential tropical cyclones. These composites show the CCKW-filtered TRMM anomalies first becoming noticeable at Day -4 over the eastern Pacific. Anomalous southerly flow begins appearing a day later and continues accelerating towards the

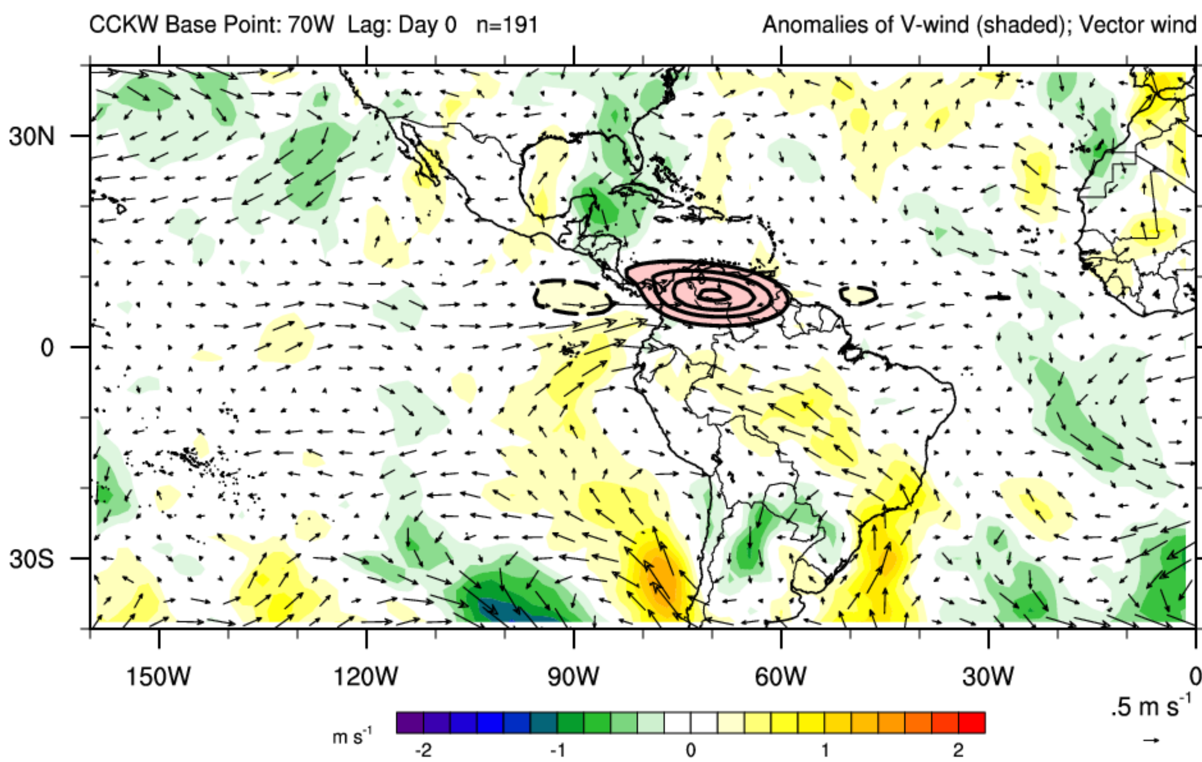

FIG. 3. Composite of total wind (vectors) and meridional wind (shading) based on positive CCKW-filtered TRMM rainfall anomalies averaged over 5-10˚N at 70˚W of at least +1 standard deviation from the period mean. Composite calculated over the July-October 1998-2010 period, which included 191 CCKW events.

equatorial Andes up through Day 0 (Fig. 3). While the complete connection into the Caribbean is not apparent in these composites, the strong southeasterly flow against the Andes can be observed, which then bends back toward the east as the terrain channels the southerly flow northward (e.g. trajectories in Fig. 1).

5. SUMMARY AND CONCLUSIONS

A standard synoptic analysis of the events that led to the genesis of the pre-Karl disturbance identified two distinct air masses that influenced the disturbance: a dry mid-level air mass sinking south and east over the subtropical Atlantic and a moistening terrain-channeled southerly flow off northern South America. The combination of these two primary air masses likely contributed to the rapid initial spin-up of the pre-Karl disturbance on 10 September and the subsequent pulsating convection as the disturbance continued to develop thereafter.

An equatorial wave perspective highlights the possible importance of some physical processes that might not otherwise be readily apparent with the pre-Karl disturbance. The initial spin-up of the disturbance appears to be associated with the passage of the western edge of the convectively active phase of an eastward-propagating CCKW, suggesting the presence of the low-level vorticity strips observed after the passage of CCKWs in the western Pacific (Schreck and Molinari 2011). When combined with a surge of southerly winds along part of this strip, a localized vortex was able to quickly form the pre-Karl disturbance.

When these two perspectives are combined, the significance of their interactions becomes clear. Increasingly moist flow off northern South America is driven by a strong southerly surge of wind from the subtropical Amazon basin during the early stages of the pre-Karl disturbance (7-11 September). This correlates well with the southerly and southeasterly flow noted in the time-lagged CCKW-centric composites (Day 0 presented in Fig. 3). In these composites, anomalous meridional flow can be seen up to 3 days prior to the arrival of the CCKW at 70˚W, which matches the observed beginning of the southerly wind surge quite well (not shown). This strong correlation between CCKW passages and southerly wind surges without a clear mid-latitude precursor indicates that some of these southerly wind surge events during the July-October period may occur via a different physical mechanism than presented by Liebmann et al (2009). Finally, a much more detailed analysis of the thermodynamics of these southerly wind surges will be necessary in order to establish what, if any, relationship exists between these winds and tropical cyclogenesis over the Caribbean Sea.

6. ACKNOWLEDGEMENTS

The authors would like to acknowledge funding provided by NSF grant AGS-0935830. Trajectory calculations were done with software written and shared by Matthew Janiga, for which we are thankful.

7. REFERENCES

Kiladis, George N., C. D. Thorncroft, N. M. J. Hall, 2006: Three-Dimensional Structure and Dynamics of African Easterly Waves. Part I: Observations. *J. Atmos. Sci.*, **63**, 2212–2230.

Liebmann, Brant, G. N. Kiladis, L. M. V. Carvalho, C. Jones, C. S. Vera, I. Bladé, D. Allured, 2009: Origin of Convectively Coupled Kelvin Waves over South America. *J. Climate*, **22**, 300–315.

Matsuno, T., 1966: Quasi-geostrophic motions in the equatorial area. *J. Meteorol. Soc. Jpn.*, **44**, 25-43.

Montgomery, Michael T., and Coauthors, 2012: The Pre-Depression Investigation of Cloud-Systems in the Tropics (PREDICT) Experiment: Scientific Basis, New Analysis Tools, and Some First Results. *Bull. Amer. Meteor. Soc.*, **93**, 153–172.

Saha, Suranjana, and Coauthors, 2010: The NCEP Climate Forecast System Reanalysis. *Bull. Amer. Meteor. Soc.*, **91**, 1015–1057.

Schreck, Carl J., and J. Molinari, 2011: Tropical Cyclogenesis Associated with Kelvin Waves and the Madden–Julian Oscillation. *Mon. Wea. Rev.*, **139**, 2723–2734.

Ventrice, Michael. J., C. D. Thorncroft, and C. J. Schreck III, 2012: Impacts of convectively coupled Kelvin waves on environmental conditions for Atlantic tropical cyclogenesis. *Mon. Wea. Rev.*, in press.

Wheeler, Matthew, G. N. Kiladis, 1999: Convectively Coupled Equatorial Waves: Analysis of Clouds and Temperature in the Wavenumber–Frequency Domain. *J. Atmos. Sci.*, **56**, 374–399.